

## 5.7. Summit, Greenland (7/12/07– 6/20/09)

This section describes quality control of solar data recorded by the SUV-150B spectroradiometer at Summit Camp, Greenland, between 7/12/07 and 6/20/09. The site visit on 7/10/07-7/12/07 marks the start of the reporting period. After season-closing calibrations on 6/19/09, the system was removed from the “Green House” as the building needed to be raised above snow level, and re-leveled. The instrument was reinstalled at the end of July 2009. Data collected in 2007 and 2008 were assigned to Volume 17; data of 2009 are part of Volume 18.

Changes in responsivity observed during the last years continued in 2008 and 2009. These changes are caused by variations in collector efficiency and PMT sensitivity. These changes are now well understood and were corrected during data processing. Residual variations in published data were assessed by comparing SUV-150B data with measurements of the co-located GUV-511 multi-filter radiometer and results of radiative transfer calculations, and are smaller than  $\pm 3\%$ , with few exceptions (Table 5.7.1).

In 2009, the Green House was almost completely snowed-in. As a consequence, irradiance collectors of the SUV and GUV were close to ground level and were frequently shaded by objects in their vicinity, including snow piles and people. Most affected data were removed from all datasets. Remaining scans were flagged in the “Version 2” dataset, but a few scans may still be part of the dataset. Periods when the collector of the GUV-511 was shaded were also excluded.

Measurements of the TSI sensor were not always correctly recorded and data from several days are missing in published databases. The Eppley PSP pyranometer (S/N 32760F3) installed next to the SUV-150B was calibrated by Eppley Laboratory on 4/8/2004. The same calibration as in the previous season was applied.

A total of 33841 scans are part of the Summit Volume 17 and 18 datasets. Only 1.2% of all possible scans were lost due to technical problems.

### 5.7.1. Irradiance Calibration

The on-site irradiance standards used during the reporting period were the lamps 200W027, 200W030, and 200W043. Lamp 200W017 served as traveling standard both at the season “opening” and “closing” site visits.

#### Calibration history of on-site standards 200W027 and 200W030

Lamps 200W027 and 200W030 were originally calibrated on 3/28/01 by Optronic Laboratories. Both lamps were recalibrated against lamp 200W017 using “closing” scans performed at Summit on 7/11/07. These calibrations were used for processing solar data of the Volume 16 period. Lamp 200W027 was temporarily moved to San Diego and was recalibrated in March 2008 against lamps 200W028 and 200W022. This calibration was used for solar data of the reporting period. Lamp 200W030 was recalibrated in June 2009 against 200W017 using “closing” scans of the Volume 18 period, which were performed at Summit on 6/19/09. This calibration was used for solar data of the reporting period. Lamp 200W043 was calibrated on 6/2/07 against a set of four FEL lamps as described below. The irradiance values assigned to lamps 200W027 and 200W030 used for calibrating solar data of the reporting period are smaller by 2.0% and 0.6%, respectively, than those applied for Volume 16 data.

Lamp 200W022 (which was used for recalibration of lamp 200W027) is one of BSI’s long-term standards and is rarely used. It was calibrated by Optronic Laboratories on 3/28/01. Lamp 200W028 is the San Diego site standard.

#### Calibration history of traveling standard 200W017 and on-site standard 200W043

Lamps 200W017 and 200W043 were calibrated in June 2007 at BSI with four 1000-Watt FEL lamps provided by the Central UV Calibration Facility (CUCF) at Boulder. This calibration procedure was

complicated by the fact that the irradiance scale of the four FEL lamps refers to the detector-based scale of the National Institute of Standards and Technology established in 2000 (NIST2000; *Yoon et al.*, 2002), whereas all solar data of the NSF UVSIMN refer to the source-based NIST scale from 1990 (NIST1990, *Walker et al.*, 1987). The NIST2000 scale is about 1.3% larger than the NIST1990 scale. Data of certificates issued by the CUCF were converted to the NIST1990 scale before the calibration was transferred to the two lamps.

Figure 5.7.1 shows a comparison of lamps 200W027, 200W030, and 200W043 with lamp 200W017 performed on 6/19/09. The three lamps are consistent with the traveling standard to within  $\pm 1\%$ . This a very good result considering that all lamps, with the exception of 200W030, have independent calibration trails. Lamps 200W027 and 200W030 were also compared with each other on 7/11/07, 9/13/08, 11/23/08, and 2/13/09. The lamps agreed with each other to within  $\pm 1.5\%$  on the first two occasions and to within  $\pm 1.0\%$  on 11/23/08 and 2/13/09.

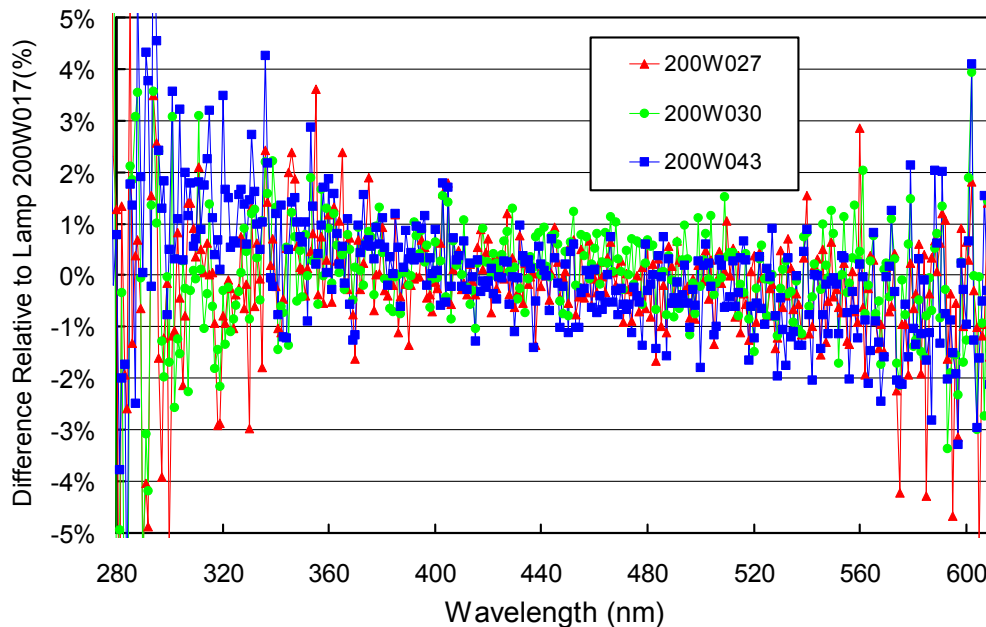


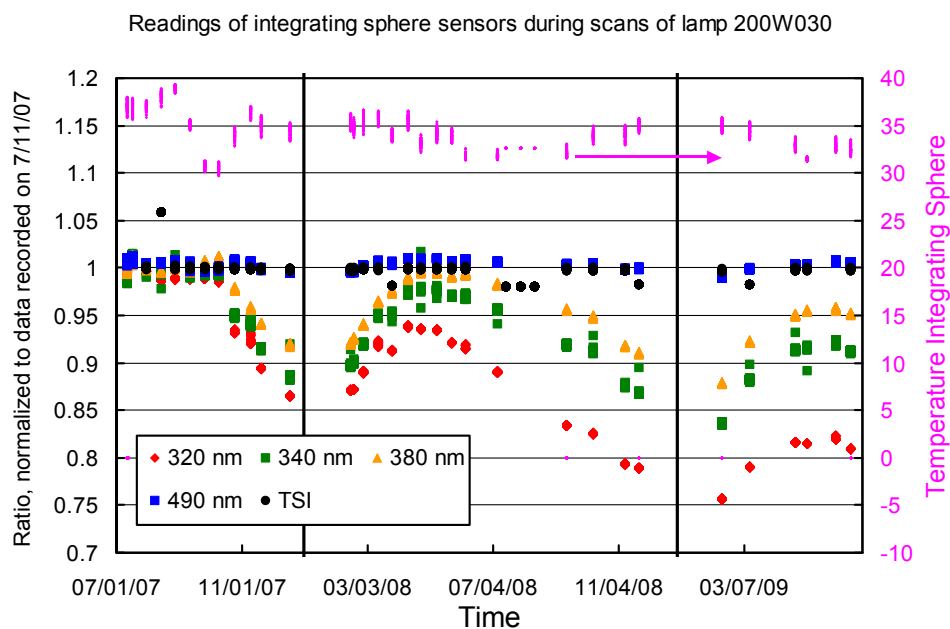
**Figure 5.7.1.** Comparison of lamps 200W027, 200W030, 200W043 with lamp 200W017. Data was collected during the site visit in June 2009.

### 5.7.2. Instrument Stability

The temporal stability of the spectroradiometer is monitored with bi-weekly calibrations utilizing site irradiance standards; daily response scans of the internal irradiance reference lamp; measurements of filtered photodiodes integral to the instrument's integrating sphere; and by comparison with the co-located GU-511 radiometer. Daily response scans help to uncover instabilities related to monochromator and PMT but cannot be used to track changes in the instrument's cosine collector (integrating sphere + PTFE diffuser). In contrast, the sphere's photodetectors are only sensitive to changes in the cosine collector and are not affected by possible drifts of other system components such as the optical fiber or the monochromator.

The stability of the cosine collector was determined by analyzing the signal of the sphere's photodetectors when executing absolute scans with lamp 200W030. Signals should ideally be constant from one calibration event to the next as the lamp was very stable. Figure 5.7.2 shows signals of the four detectors, plus the TSI sensor, as a function of time. Data were normalized to signals recorded during the first

absolute scan, performed on 7/11/07. Results indicate that the throughput of the collector was constant up to 10/9/07, before it started to decrease in the UV. Changes are largest at shortest wavelength (320 nm). The minimum was observed during the last scan of 2007, performed on 12/18/07. Between January and April 2008, the throughput increased again, it remained fairly constant between May and June, and decreased thereafter. The pattern in 2009 resembles that of 2008, however, the throughput in the UV was smaller at the end of the reporting period compared to the beginning even though start and end date are during the same part of the year. Changes of similar magnitude have also been reported in the Volume 15 and 16 Operations Report. We attribute these partially reversible drifts to changes in the reflectivity of the integrating sphere's wall, but the detailed mechanism is still unknown. The throughput is generally smaller during the darkest part of the year, indicating that the changes may be caused by light sensitization. Results are consistent with the analysis of absolute scans (Figures 5.7.4.a - 5.7.4.d), excluding the possibility that drifts are caused by changes in the sensitivity of the photodetectors. Changes of the sphere's throughput are generally well predictable and could be corrected.



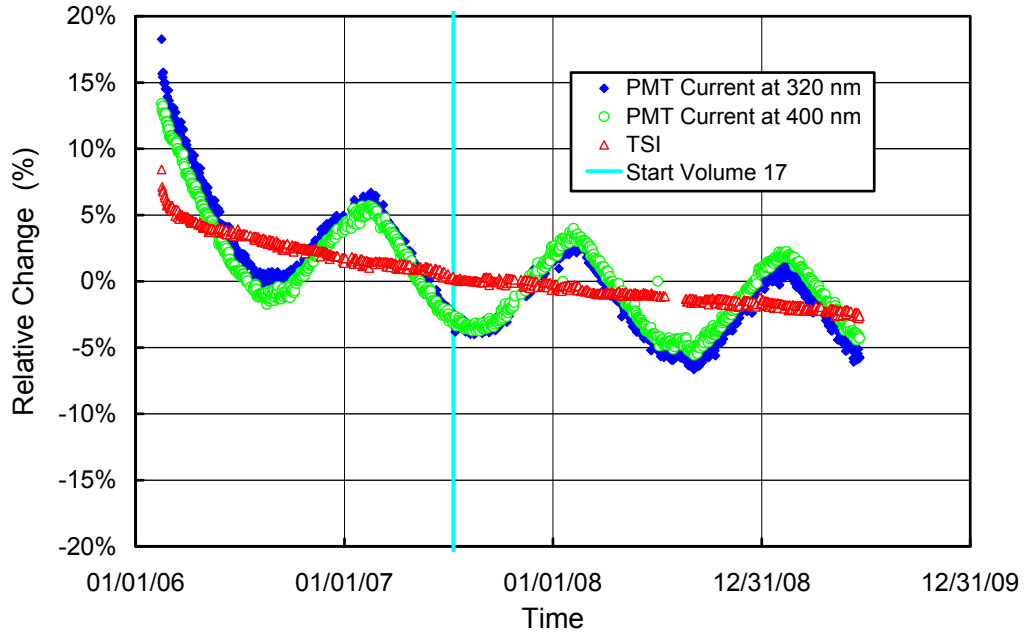
**Figure 5.7.2.** Analysis of change in throughput of the instrument's integrating sphere. Change was assessed by analyzing data of photodetectors that are mounted around the sphere's exit port plus the TSI sensor. Signals of the detectors were recorded during absolute scans with lamp 200W030. Measurements are normalized to data recorded on 7/11/07. Vertical lines indicate 1/1/08 and 1/1/09.

Figure 5.7.3 shows changes in TSI readings and PMT currents at 320 and 400 nm, derived from response scans performed between 12/14/06 and 6/20/09. TSI measurements changed by less than 10% over this 3.5-year long period, indicating very good stability of the internal lamp. In particular since April 2006, the change of the lamp was very predictable. PMT currents exhibit a distinct annual cycle with an amplitude of about  $\pm 5\%$ . The highest PMT sensitivity is observed in mid-February of every year, while the lowest sensitivity is observed in August. We attribute this periodicity to long-term memory of the PMT to the radiation levels it has "seen" during the months prior to the measurement. During the period of winter darkness, the PMT becomes more sensitive, and during the summer months the sensitivity decreases. As the variation is very predictable, it can be well corrected during data processing.

To account for changes of the system's responsivity sphere-throughput and PMT-sensitivity, the reporting period was broken into 33 sub-periods and a different irradiance spectrum was applied to the internal lamp in each period. A summary of the calibration periods is provided in Table 5.7.1. The ratio of these irradiance spectra relative to the spectra applied in periods P1, P7, P12, and P18 are shown in Figures 5.7.4.a - 5.7.4.d, respectively.

**Table 5.7.1. Calibration periods for Summit Volumes 17 and 18.**

Period name	Period range	Number of absolute scans	Remarks
P1		2	Season opening - not used
P2	07/12/07 - 09/17/07	5	
P3	09/18/07 - 10/13/07	2	Ratio GUV/SUV @340 nm low by ~2.5%
P3B	10/14/07 - 10/20/07	0	Interpolated from periods P3 and P4 Ratio GUV/SUV @340 nm low by up to 5%
P4	10/21/07 - 11/01/07	1	
P5	11/02/07 - 11/14/07	1	
P6	11/15/07 - 12/31/07	1	
P7	01/01/08 - 01/28/08	1	
P7B	01/29/08 - 02/09/08	0	Interpolated from periods P7 and P8
P8	02/10/08 - 02/22/08	2	Ratio GUV/SUV @340 nm low by up to 3.5%
P9	02/23/08 - 03/06/08	1	Ratio GUV/SUV @340 nm low by up to 4%
P10	03/07/08 - 03/21/08	1	
P11	03/22/08 - 04/01/08	1	
P11B	04/02/08 - 04/09/08	0	Interpolated from periods P11 and P12
P12	04/10/08 - 06/22/08	5	
P13	06/23/08 - 07/20/08	2	
P13B	07/21/08 - 07/27/08	0	Interpolated from periods P13 and P14
P14	07/28/08 - 09/01/08	3	Ratio GUV/SUV @340 nm high by ~2%
P14AA	09/02/08 - 09/08/08	0	Interpolated from periods P14 and P14A
P14A	09/09/08 - 09/28/08	3	
P14B	09/29/08 - 10/05/08	0	Interpolated from periods P14A and P15
P15	10/06/08 - 10/14/08	1	
P15B	10/15/08 - 10/21/08	0	Interpolated from periods P15 and P16
P15C	10/22/08 - 10/25/08	0	Interpolated from periods P15 and P16
P16	10/26/08 - 11/09/08	1	Scaled up by 1.5%
P17	11/10/08 - 12/31/08	4	
P18	01/01/09 - 02/16/09	4	
P18B	02/17/09 - 02/23/09	0	Interpolated from periods P18 and P19
P19	02/24/09 - 03/02/09	1	
P20	03/03/09 - 04/04/09	2	Ratio GUV/SUV @340 nm low by up to 4%
P20B	04/05/09 - 04/19/09	0	Interpolated from periods P20 and P21 Ratio GUV/SUV @340 nm low by up to 4%
P21	04/20/09 - 05/01/09	1	
P22	05/02/09 - 06/20/09	7	



**Figure 5.7.3.** Time-series of TSI signal and PMT currents at 320 and 400 nm during measurements of the internal reference lamp performed at Summit between 2/15/06 and 6/20/09.

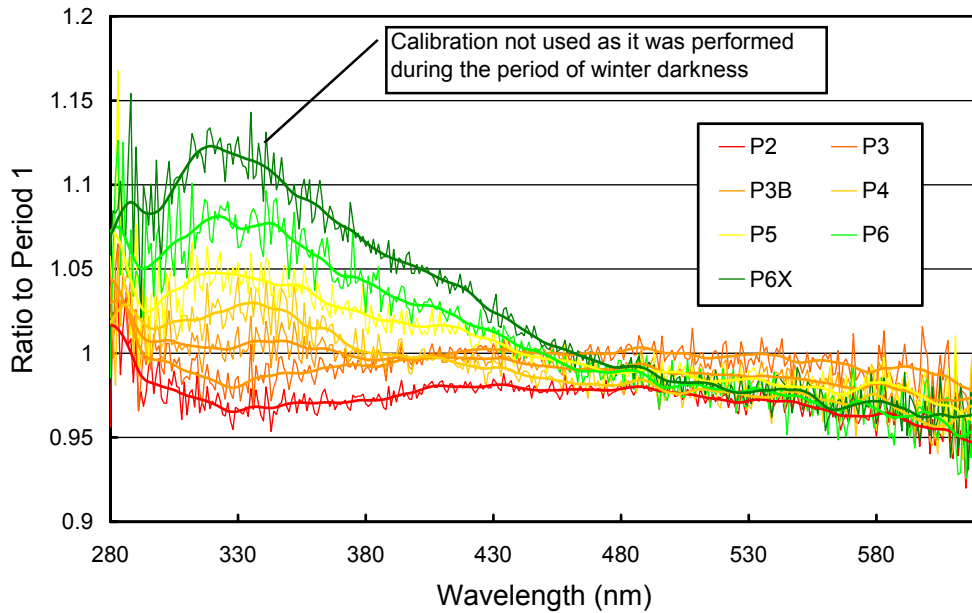


**Figure 5.7.4.a** Ratios of irradiance assigned to the internal reference lamp in Periods P2 – P6X, referenced to the irradiance of Period P1. Data cover the period 7/12/07 - 12/31/07.

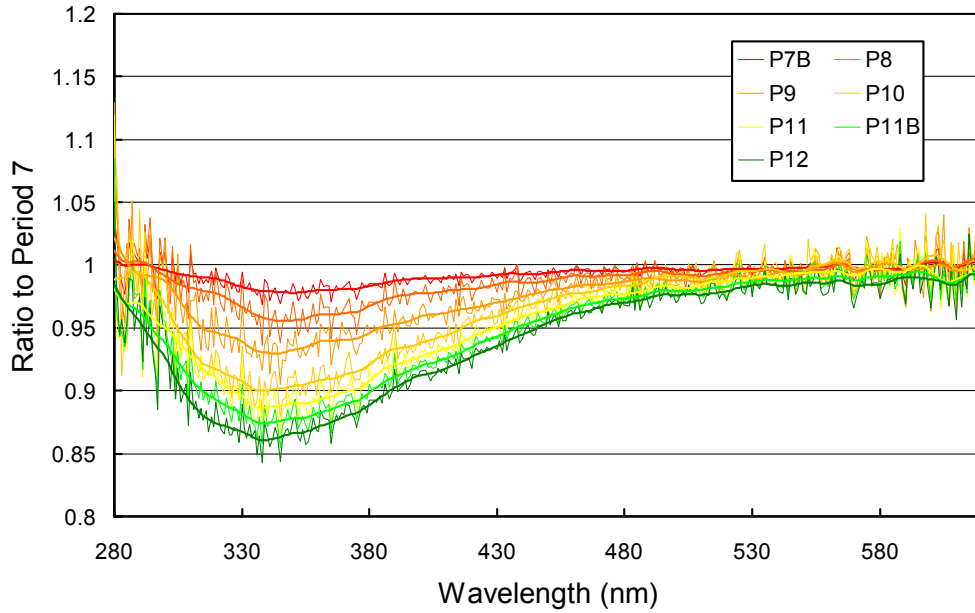


**Figure 5.7.4.b** Ratios of irradiance assigned to the internal reference lamp in Periods P7B – P12, referenced to the irradiance of Period P7. Data cover the period 1/1/08 - 6/22/08.

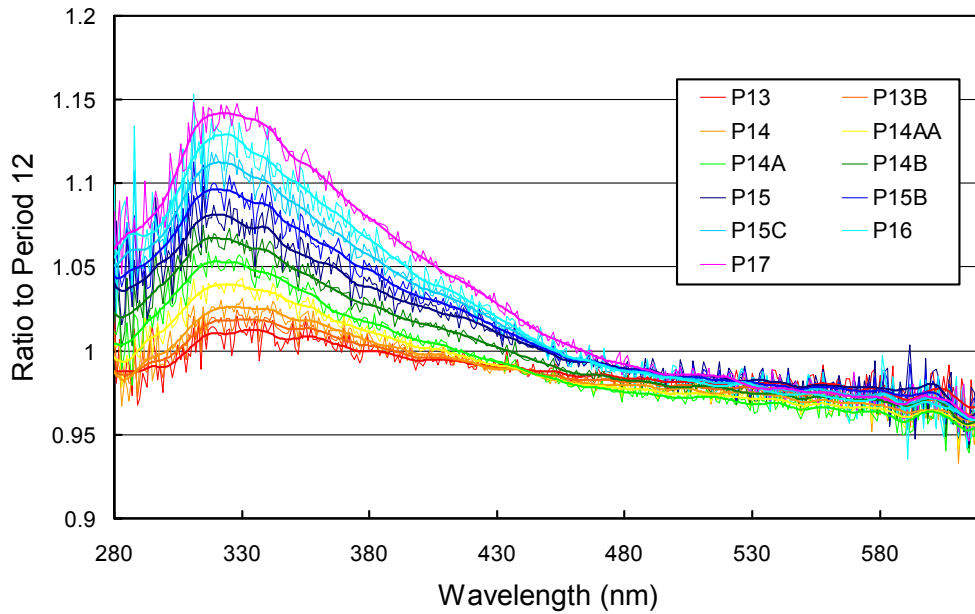


**Figure 5.7.4.c** Ratios of irradiance assigned to the internal reference lamp in Periods P13 – P17, referenced to the irradiance of Period P12. Data cover the period 4/10/08 - 12/31/08.

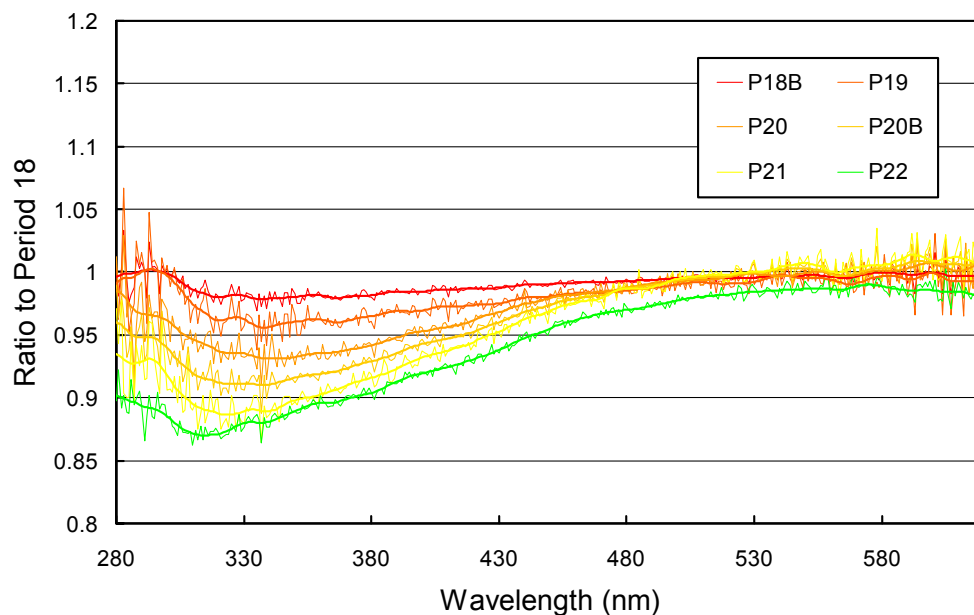


**Figure 5.7.4.d** Ratios of irradiance assigned to the internal reference lamp in Periods P18B – P22, referenced to the irradiance of Period P18. Data cover the period 1/1/09 - 6/20/09.

The quality of calibrated solar measurements of the SUV-150B was further assessed by comparison with the GUV-511 radiometer. Figures 5.7.5.a - 5.7.5.c show the ratio of measurements of the GUV's 340 nm channel to measurements of the SUV-150B. The latter have been weighted with the spectral response function of the GUV's channel prior to forming the average. Data from 2007, 2008, and 2009 are shown in separate figures. Measurements of the two instruments agree to within  $\pm 5\%$ , with the exception of a few outliers, which are discussed further below. The standard deviation of the ratio is 1.8%. Some outliers were caused by snow accumulation on either or both of the two instrument collectors, particularly in 2009. Affected data were removed from the published dataset. Step-changes at times when the SUV's calibration was changed are typically smaller than 2.5%, but step changes of 2-4% are observed between Periods P3B and P4, P8 and P9, P9 and P10, P20 and P20B, and P20B and P21. Periods when the uncertainty of SUV data is increased due to changes in the instrument's responsivity are generally those periods when the ratio of GUV/SUV at 340 nm exceeds  $\pm 2\%$ . These periods are also indicated in Table 5.7.1. Uncertainties in the visible are smaller than in the UV due to the spectral pattern of changes in the sphere throughput.

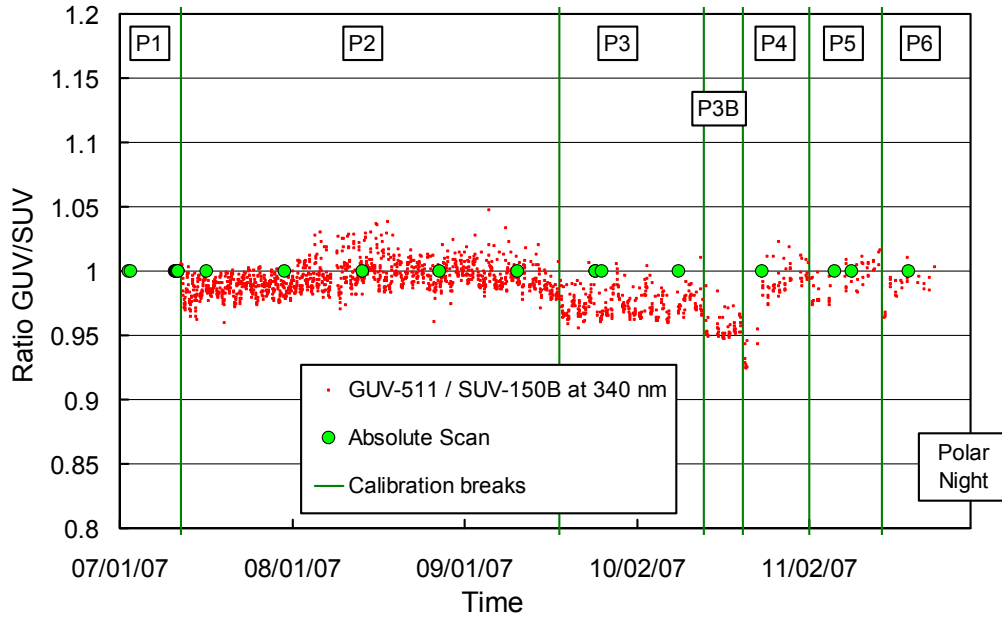


Figure 5.7.5.a. Ratios of GUV-511 and SUV-150B measurements at 340 nm for 2007.

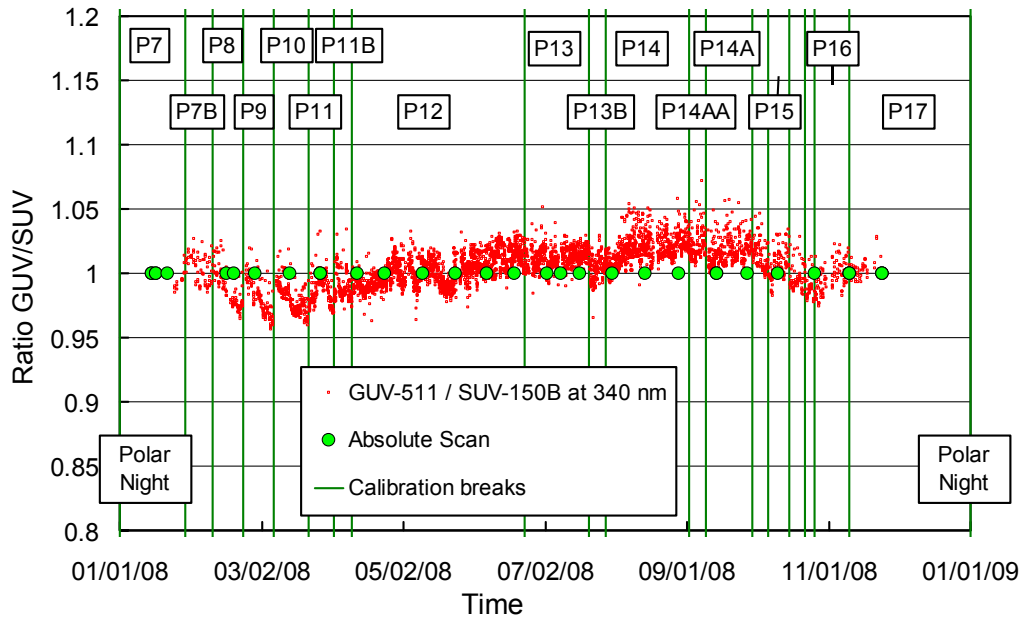
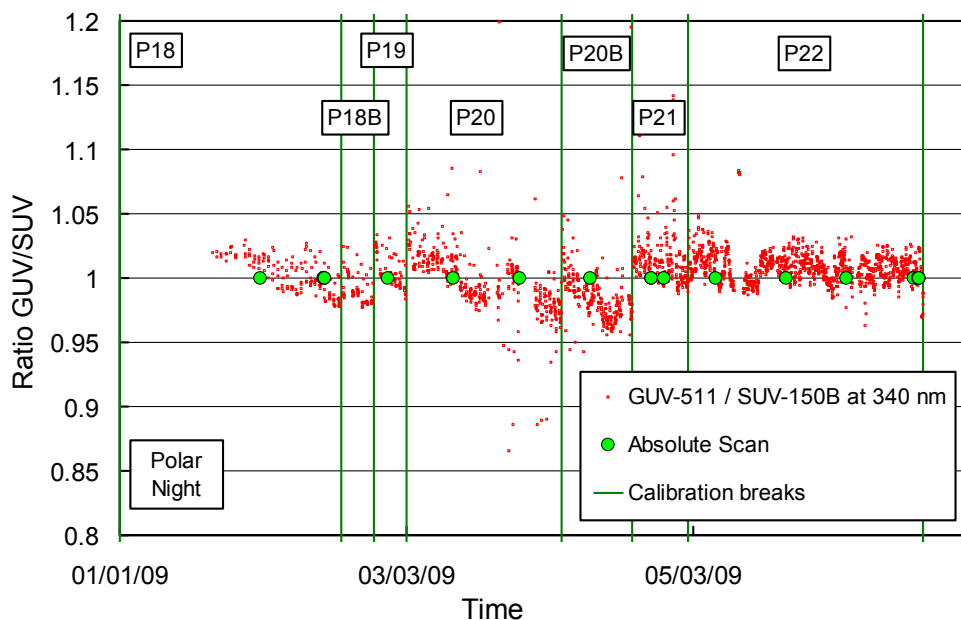


Figure 5.7.5.b. Ratios of GUV-511 and SUV-150B measurements at 340 nm for 2008.





**Figure 5.7.5.c.** Ratios of GUV-511 and SUV-150B measurements at 340 nm for 2009.

### 5.7.3. Wavelength Calibration

Wavelength stability of the system was monitored with the internal mercury lamp. Figure 5.7.6 shows the differences in the wavelength offset of the 296.73 nm mercury line between pairs of consecutive wavelength scans for the period 7/12/07 – 6/20/09. In total, 664 scans were evaluated. For 99.85% of the scans is the difference in the wavelength offset to neighboring scans less than  $\pm 0.0055$  nm. Note that this stability is a factor of 10 better than the wavelength stability of SUV-100 spectroradiometers. The SUV-150B has a superior wavelength stability due to the use of high-resolution optical encoders that are used in a closed feedback loop with the stepper-motor controllers.

After the data was corrected for day-to-day wavelength fluctuations, the wavelength-dependent bias between this homogenized data set and the correct wavelength scale was determined with the Fraunhofer-line correlation method used for Version 2 processing (Bernhard *et al.*, 2004; see also Section 4.2.2.2). Due to the good wavelength stability of the system, only one correction function had to be applied for the entire reporting period. This function is shown in Figure 5.7.7. Since the positions of the monochromator's gratings are determined by optical encoders, irregularities in the monochromator drive are inconsequential. This explains the smoothness of the function. Most of the variations observed are artifacts of the correlation algorithm, which has an uncertainty of about 0.015 nm.

After data was corrected using this function, the wavelength accuracy of all noontime scans was verified with the "Version 2" Fraunhofer-line correlation algorithm. The results are shown in Figure 5.7.8 for four UV wavelengths and one wavelength in the visible. Residual shifts are typically smaller than  $\pm 0.03$  nm. A more detailed analysis reveals that wavelength shifts at 320 nm are smaller than  $\pm 0.02$  nm for 96% of all scans. A few outliers occur when spectra are affected by changing cloud cover. The wavelength stability is not worse during cloudy conditions, but the validation is subject to larger uncertainties.

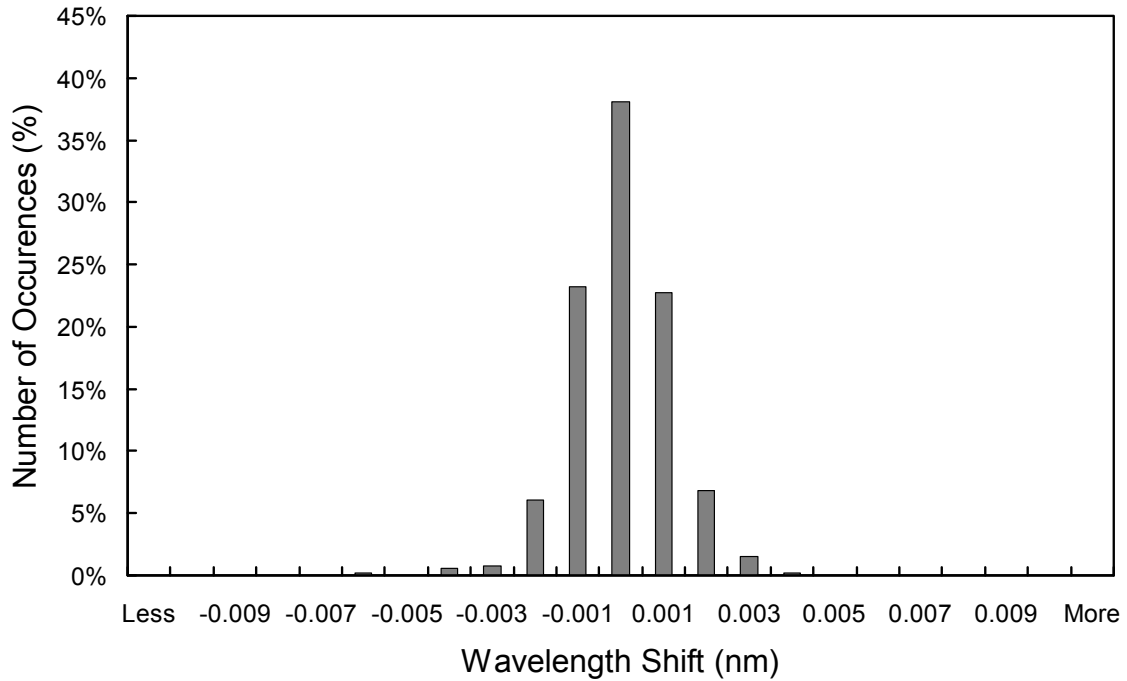


**Figure 5.7.6.** Differences in the measured position of the 296.73 nm mercury line between consecutive wavelength scans for the period 7/12/07 – 6/20/09. The labels of the horizontal axis give the center wavelength shift for each column. The 0-nm histogram column covers the range from -0.0005 to +0.0005 nm. “Less” means shifts smaller than -0.0105 nm; “more” means shifts larger than 0.0105 nm.

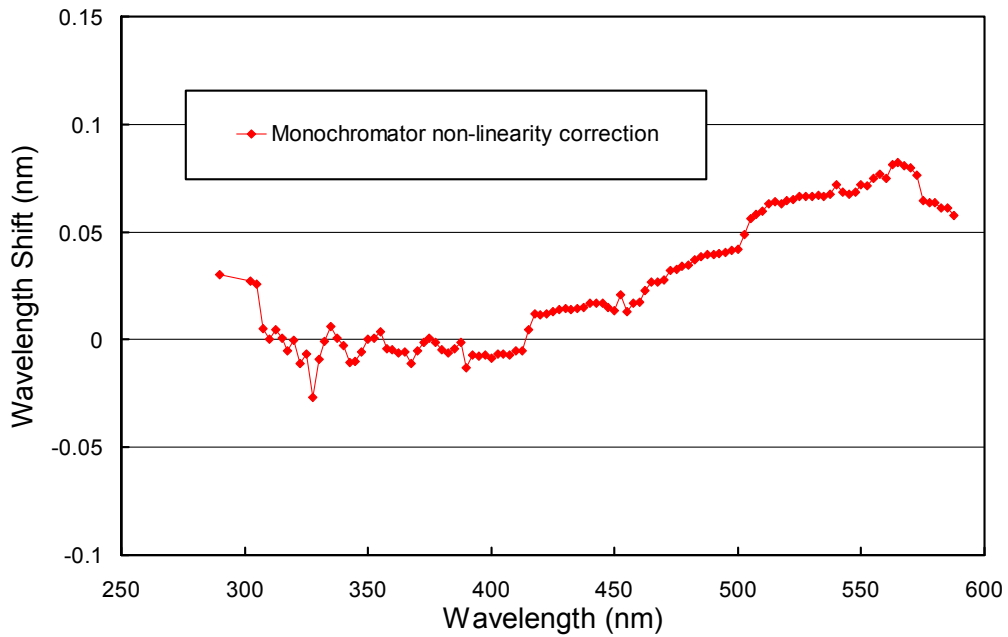


**Figure 5.7.7.** Monochromator non-linearity correction functions for Volume 16 and 17 periods at Summit.

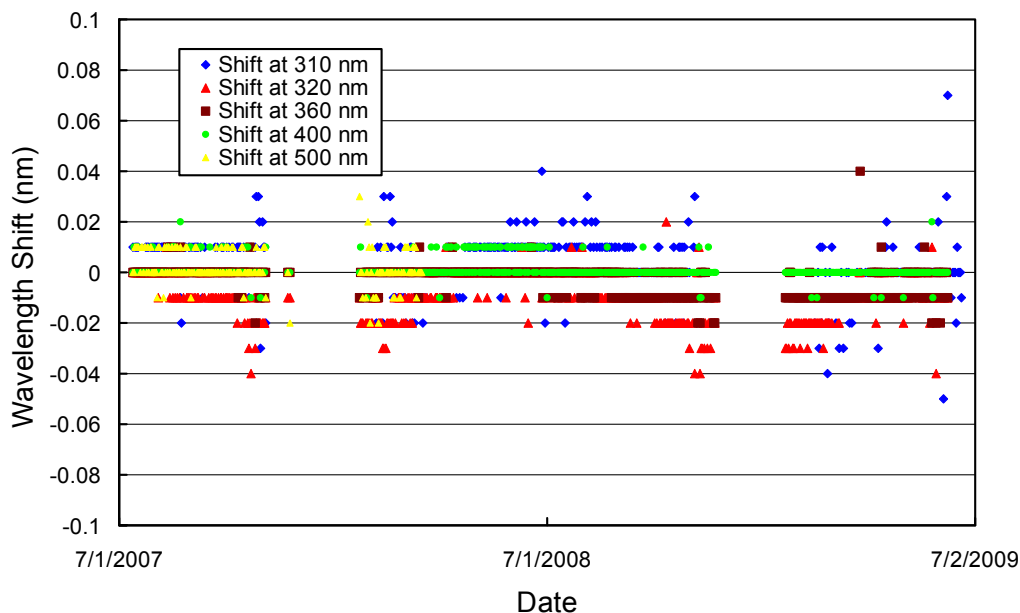


**Figure 5.7.8.** Wavelength accuracy check of final data at five wavelengths in the UV and visible by means of Fraunhofer-line correlation. All noontime measurement have been evaluated.

#### 5.7.4. Missing Data

A total of 33841 scans are part of the Summit Volume 17 and 18 datasets. Only 1.2 % of all possible scans were lost due to technical problems. 0.8% of all scans that were affected by snow accumulation close to the detector of the system had to be removed from the datasets. Missing periods are summarized in Table 5.7.2.

**Table 5.7.2. Missing solar scans in the Summit Volume 17 and 18 datasets.**

Period	Number of scans	Reason
<i>Calibration scans</i>		
Throughout season	1094	Response scans
Throughout season	695	Wavelength scans
Throughout season	208	Absolute scans
<i>Operational support</i>		
04/03/08	16	Operator training
<i>Technical problems</i>		
Throughout season	12	Scans found defective
09/24/07	22	Electrometer not responsive
10/23/07	24	Software error
02/17/08	9	Software error
02/28/08	27	Software error
07/08/08	7	GPS problem
07/30/08	30	Outlier for unknown reasons
08/17/08 - 08/18/08	96	Software error
10/30/08 - 10/31/08	56	Measurements affected by snow accumulation
11/01/08	24	Problem with data acquisition unit

11/18/08 - 11/19/08	14	Software error
03/18/09	30	Measurements affected by snow accumulation
03/20/09 - 03/24/09	159	Measurements affected by snow accumulation
04/08/09 - 04/09/09	53	Measurements affected by snow accumulation
05/11/09 - 05/12/09	90	Power outage
05/20/09	69	Problem with GPS
05/28/09	10	Power outage

### 5.7.5. GUV Data

The GUV-511 radiometer, which is installed next to the SUV-150B, was calibrated against final SUV-150B measurements following the procedure outlined in Section 4.3.1. From the calibrated measurements, data products were calculated (Section 4.3.2). Figure 5.7.9 shows a comparison of GUV-511 and SUV-150B erythemal irradiance based on final Volume 17 and 18 data. For solar zenith angles smaller than  $80^\circ$ , measurements of the two instruments agree to within  $\pm 1.5\%$  ( $\pm 1\sigma$ ). This good agreement confirms that drifts in SUV-150B data discussed in Section 5.7.2 have been satisfactorily removed by adjusting the instrument's calibrations. We advise data users to use SUV-150B rather than GUV-511 data whenever possible, in particular for low-Sun conditions.

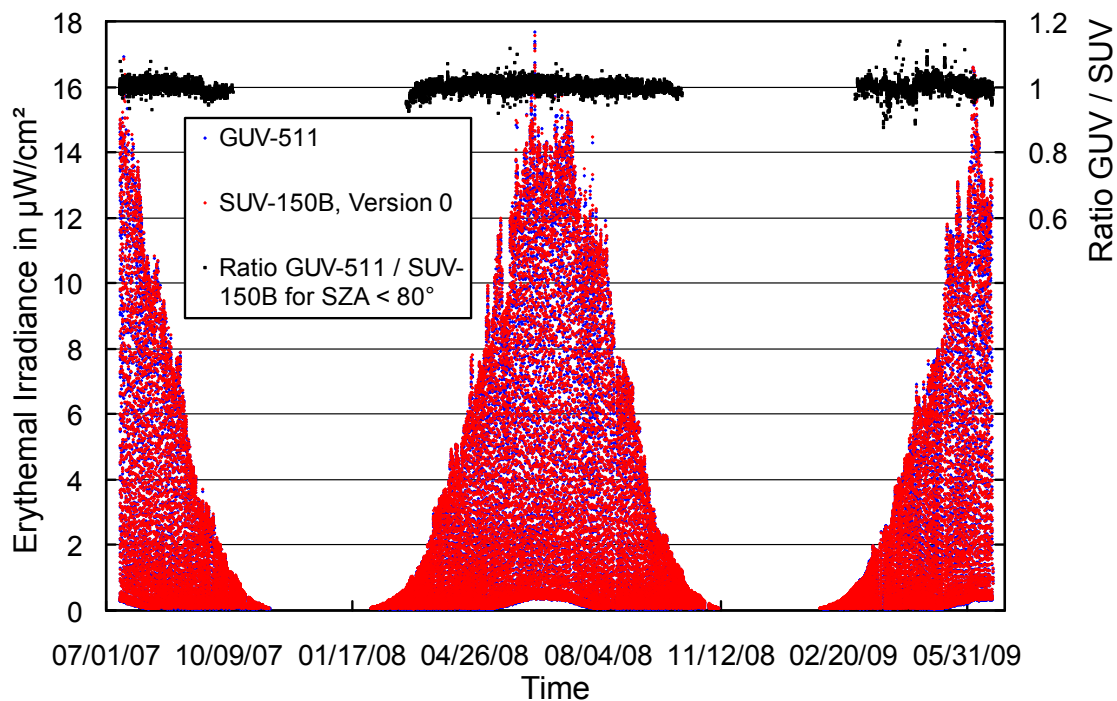


**Figure 5.7.9.** Comparison of erythemal irradiance measured by the SUV-150B spectroradiometer and the GUV-511 radiometer. SUV-150B measurements are based on “Version 0” (cosine-error uncorrected) data.

Figure 5.7.10 shows a comparison of total ozone measurements from the GUV-511, the SUV-150B (Version 2 data, available at [www.biospherical.com/nsf/Version2/](http://www.biospherical.com/nsf/Version2/)), and the Ozone Monitoring Instrument (OMI). GUV-511 ozone values were calculated as described in Section 4.3.3. Between May and September, GUV-511 ozone data agree almost ideally with SUV-150B and OMI measurements. GUV data

are a few percent low for March, April, and October when solar elevations are small. The reason for this bias is the effect of the ozone profile on ozone retrievals. For SZA larger than  $80^\circ$ , measurements of the GUV's 305 nm channel are close to the detection limit. GUV ozone data at large SZAs become unreliable and should not be used. There is generally good agreement between SUV-150B and OMI data. The average ratio SUV/OMI is 1.015, and the standard deviation of the two datasets is 4.1%. This good agreement—even at large SZAs—is achieved by using ozone profiles in the inversion algorithm, which were measured at Summit by NOAA/ESRL.

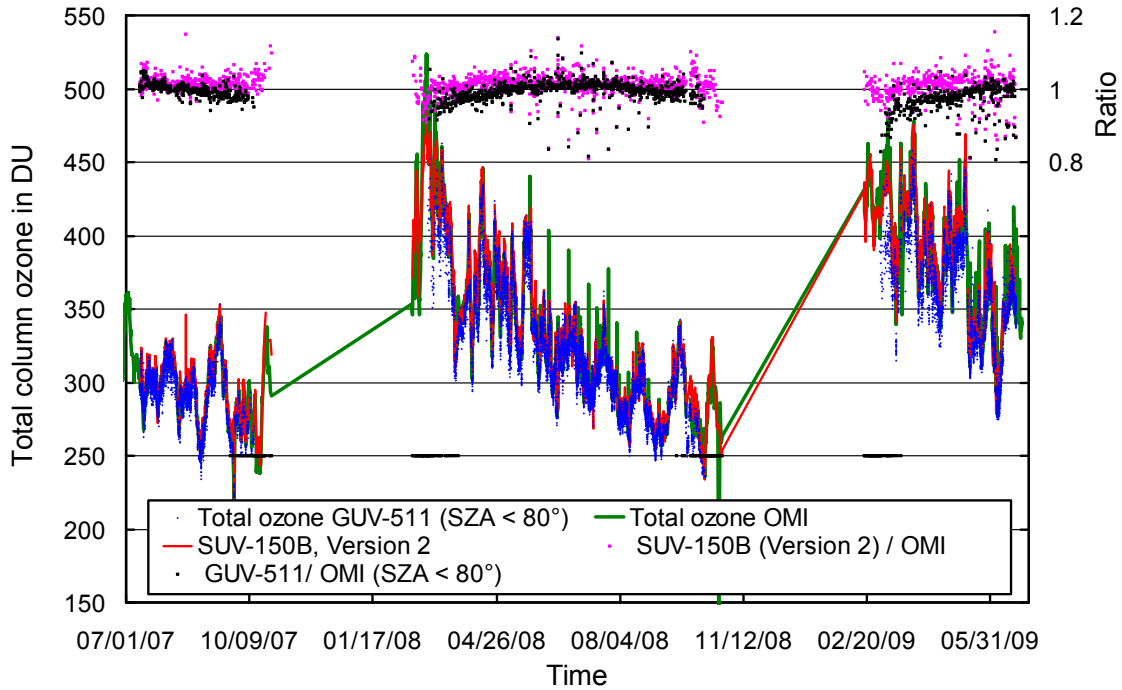


**Figure 5.7.10.** Comparison of total column ozone measurements from GUV-511, SUV-150B (Version 2 data), and OMI. GUV-511 measurements are plotted in 15 minute intervals. For calculating the ratio of data sets, only measurements concurrent with the OMI overpass were evaluated.